Self-organizing fault systems and self-organizing elastodynamic events on them: Geometry and the distribution of sizes of events

Bruce E. Shaw

Lamont-Doherty Earth Observatory, Columbia University, New York, USA

[1] We introduce a new model which both generates a self-organizing complex segmented fault system which then accommodates finite strain, and generates sequences of elastodynamic events on that complex fault system. This opens up a new realm of study of populations of cascading elastodynamic ruptures on complex fault systems. We examine the distribution of sizes of events in the model, and its dependence on fault geometry. We see an evolution from a more Gutenberg-Richter like distribution of events at smaller strains to a more characteristic like distribution at larger strains. We see relative insensitivity of the distribution of sizes of events to the friction used. Examining the distributions of sizes of events on fault segments of different lengths, we find support for a modified segmentation hypothesis whereby segments both break in power law small events and occasionally participate in cascading multisegment larger ruptures, but also predominantly break as a unit. *INDEX TERMS:* 7209 Seismology: Earthquake dynamics and mechanics; 7230 Seismology: Seismicity and seismotectonics; 7260 Seismology: Theory and modeling; 8010 Structural Geology: Fractures and faults; 8109 Tectonophysics: Continental tectonics—extensional (0905). **Citation:** Shaw, B. E. (2004), Self-organizing fault systems and self-organizing elastodynamic events on them: Geometry and the distribution of sizes of events, *Geophys. Res. Lett.*, *31*, L17603, doi:10.1029/2004GL019726.

1. Introduction

[2] The Gutenberg-Richter law for the distribution of sizes of events, stating that earthquakes follow a power law distribution of sizes of events, is one of the most important and ubiquitous observations in seismology. If one looks in detail at it, however, interesting issues emerge. While the law describes the complete population of events, the distributions of events on the individual faults which make up the whole fault system remains an open question. One extreme posits that each fault segment breaks with some characteristic size event, and it is the distribution of sizes of faults which then leads to the distribution of sizes of events. An alternative extreme posits that each fault itself produces a power law distribution of sizes of events, and it is the dynamics of individual faults which underlie the distribution of sizes of events. Other positions link these extremes, e.g., through the evolution of fault properties over geological timescales, with faults evolving from young rough faults with power law distributions towards more mature smooth faults with more characteristic distributions

[*Stirling et al.*, 1996]. To get at these issues from a theoretical point of view, we need to tackle both the issue of fault system geometry, and event dynamics, over many earthquake cycles.

[3] Here, we present a new model which both generates self-consistent complex fault geometries, and generates self-consistent elastodynamic events on those geometries. Further, because of the numerical efficiency of the model, we can generate long sequences of events, and study the statistics of the populations. With this model, we can thus begin to address the fundamental questions of the interaction of geometry and dynamics. In this letter, we present this new model, and its application to the issue of fault geometry and the distribution of sizes of events.

[4] Previous work has examined the evolution of populations of events on complex fault systems; these approaches have, however, neglected the dynamics on the rupture timescale, simplifying the interactions to be quasi-static [*Lyakhovsky et al.*, 2001]. Other models have treated elastodynamic event populations, but only with simple fault geometries [*Carlson and Langer*, 1989; *Myers et al.*, 1996]. Other models have examined individual elastodynamic events on nonplanar fault geometries, but not populations of events [*Harris et al.*, 1991; *Kame and Yamashita*, 1997; *Bouchon and Streiff*, 1997]. One modeling approach has looked at event sequences on an individual complex fault [*Mora and Place*, 1999]. With our new model, we open up a new regime of study, of elastodynamic event sequences on complex fault systems.

2. The Model

[5] Our model involves the integration of two separate parallel modeling efforts. In one effort, we have studied sequences of elastodynamic ruptures on simple planar faults. This work, in both two dimensions and three dimensions, has shown that a rich complex population of events can arise from the dynamics alone, a population with many earthquake like properties. [*Myers et al.*, 1996; *Shaw*, 1998; *Shaw and Rice*, 2000; *Shaw and Scholz*, 2001].

[6] The fault systems work modeled the growth of faults in an extensional setting, with the stretching of a brittle layer overlying a ductile layer. The simplified two dimensional scalar model produced a growing population of normal faults, with fault systems which evolved with increasing strain. Figure 1 shows an example of the fault systems which develop [*Spyropoulos et al.*, 2002]. The self-organizing faults keep the accumulating stresses finite and self-consistent even with finite deformations.

[7] Combining these two lines of research, we are now able to simulate sequences of elastodynamic events on these

complex fault systems. Crucially, we are able to simulate long sequences of events. This is essential, because the size of an individual event depends not only on the geometry of the fault and the frictional properties on the fault, but the stress field an event propagates through [*Harris et al.*, 1991; *Harris and Day*, 1999]. Because this stress field arises from the stress field left over by previous events, we therefore need to evolve the system for a long enough time so it can reach the dynamical attractor, where the geometry and the friction and the stress field are all then self-consistent.

[8] The model equations for the bulk consist of a 2D Klein-Gordon equation for the displacement field of the upper brittle layer coupled to a lower layer stretching uniformly in one direction [*Spyropoulos et al.*, 2002]. When stress exceeds the strength at a point, a dislocation occurs, adding slip to a fault if slip has occurred there previously or creating a new fault if there was no prior slip there. For numerical simplicity, we restrict the faults to form perpendicular to the stretching direction, and discretize the equations on a rectangular lattice. Our advance here over prior work [*Spyropoulos et al.*, 2002], is that we consider fully inertial dynamics in the bulk, and dynamic strength weakening on the faults, so that now brittle deformation occurs through a self-organizing population of elastodynamic events.

[9] All of the nonlinearity in the problem is in how the fault strength evolves. (The linear bulk equations, which couple to the strength as a boundary condition on a fault, are reproduced in an electronic supplement[1], and implicitly in *Spyropoulos et al.* [2002]). This frictional strength of faults remains a big open question. While there are reasons for thinking we may have a pretty good handle on what is happening at slow slip rates [*Dieterich*, 1994; *Heslot et al.*, 1994], at high slip rates things are extremely uncertain, and many potential physical effects may be occurring, with substantially different implications for friction [*Sibson*, 1973; *Melosh*, 1996; *Rice*, 1999; *Tullis and Goldsby*, 2003]. With friction at high slip rates being an open question, we use a friction which has a minimum of parameters, is computationally efficient, and spans a range of frictional instabilities, including slip-, time-, and velocity-weakening [*Shaw*, 1995; *Shaw and Rice*, 2000]. Specifically, we use a Φ which combines long term geological strength Φ_S which weakens with accumulated geological slip [*Spyropoulos et al.*, 2002] and a dynamic strength Φ_Q which weakens during events [*Shaw*, 1997]

$$\Phi = \Phi_S + \Phi_Q. \tag{1}$$

The long term strength is given by

$$\Phi_S = \Phi_0 + \xi - \frac{\beta S}{1 + aS}. \tag{2}$$

Here Φ_0 is a constant overall strength which is irrelevant to the problem, ξ is a random variable of amplitude between 0 and ξ_0, varying in space but fixed in time. This seeds some initial random strength heterogeneity in the model. Geological slip weakening occurs with the last term, which

[1]Auxiliary material is available at ftp://ftp.agu.org/apend/gl/2004GL019726.
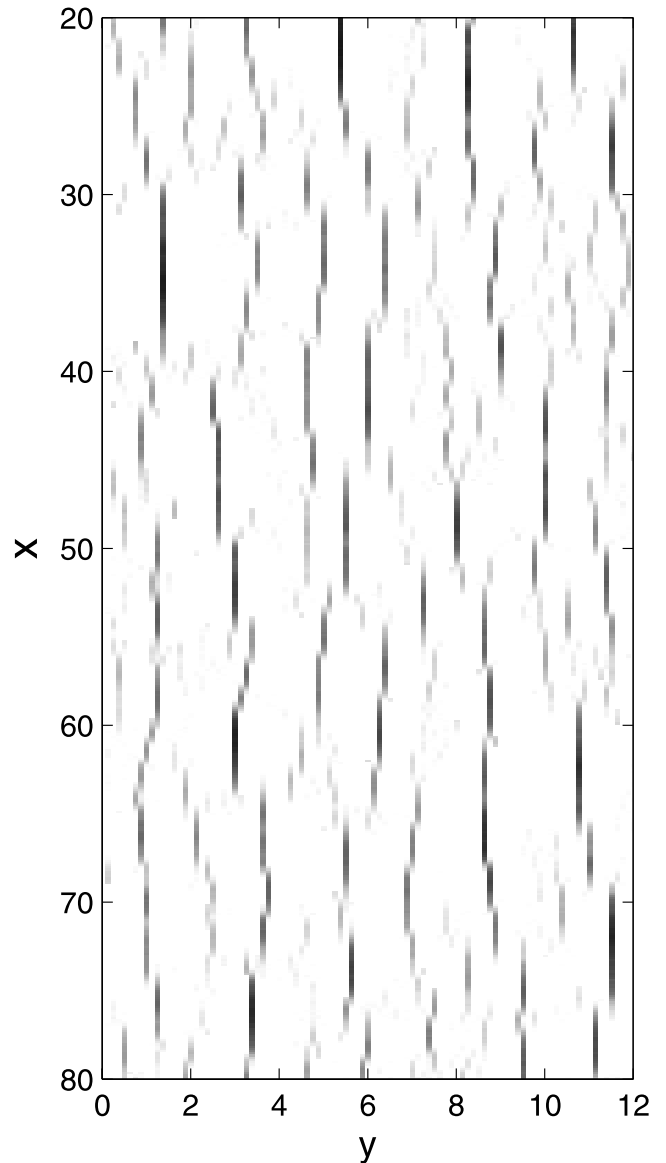
Figure 1. Plan view of faults. Greyscale is proportional to slip. Only recently active faults are shown. Note association of small scale faulting with large segment stepovers and terminations. y direction parallel to stretching, x direction perpendicular to stretching; lengths scaled to brittle layer depth.
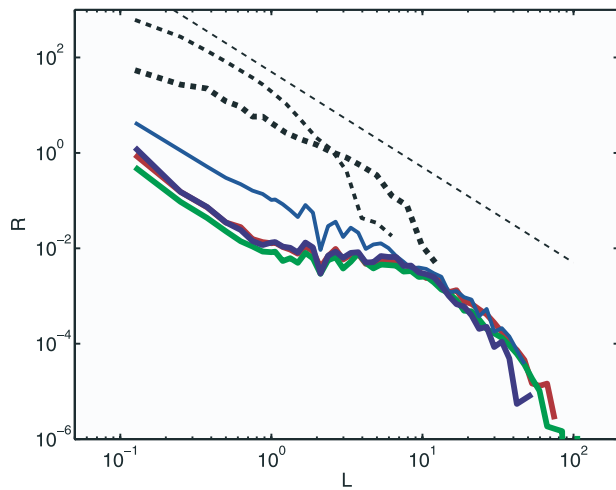
is proportional to slip S with a constant β. β affects the degree of localization in the problem, and therefore the resulting fault geometry. For large Φ_0, we can operate in a regime where the saturating term a is small and irrelevant. The brittle strain excess $\varepsilon \equiv (\nu t - \Phi_0)/\xi_0$ gives the relevant strain [*Spyropoulos et al.*, 2002]; this shows as well why Φ_0 is irrelevant, since it can be scaled out by the loading νt.

[10] For the dynamic strength weakening, we consider three terms

$$\Phi_Q = -\frac{\alpha Q}{1 + \alpha Q} - \Sigma_t - \epsilon \nabla_\parallel^2 \frac{\partial S}{\partial t} \tag{3}$$

The first term, which is a function of heat Q, models frictional weakening from frictional heating; pore fluid

Figure 2. Distribution R of lengths L of events for different fault geometries. Two different geometries are shown, one at lower strain ($\varepsilon = 0.8$) and one at higher strain ($\varepsilon = 2$), shown with the thinner and thicker lines, respectively. At each strain, we plot the distribution of lengths of events with solid lines, and the distribution of lengths of segments with dotted lines. Three different frictions are shown for the higher strain value, shown with different color curves, with slip weakening (blue line; $\alpha = 3$ $\gamma = .1$), velocity weakening (red line; $\alpha/\gamma = 3$ $\gamma = 3$), and time weakening (green line; $\alpha = 0$ $\sigma_0 = 1.3$) plotted. Note the very small difference between the different color thick curves, in contrast with the significantly larger difference between the different thickness curves, indicating that the distributions are relatively insensitive to the frictions used, but do depend on the strain and thus fault geometry. Note the more characteristic like distribution of sizes of events at the larger strain. Note also that the distribution of lengths of events is not a simple scaling of the distribution of lengths of segments. The thin black dashed line has a slope of -2 for comparison.

effects [*Sibson*, 1973; *Lachenbruch*, 1980; *Shaw*, 1995] and flash heating of asperities [*Rice*, 1999] are two potentially relevant physical mechanisms which this simplified quantification could represent. The weakening rate constant α is a critical parameter in many aspects of the dynamics, although the results we present here are mainly insensitive to it. Heat accumulates with slip rate, and dissipates over some timescale $1/\gamma$:

$$\frac{\partial Q}{\partial t} = -\gamma Q + \left|\frac{\partial S}{\partial t}\right|. \qquad (4)$$

Slip weakening results from $\gamma \ll 1$, while velocity weakening results from $\gamma \gg 1$ [*Shaw*, 1995; *Shaw and Rice*, 2000].

[11] The second term in equation (3)

$$\Sigma_t = \begin{cases} \sigma_0 \dfrac{t - t_s}{t_0} & t - t_s < t_0; \\ \sigma_0 & t - t_s \geq t_0. \end{cases} \qquad (5)$$

is a nucleation term, which we make a big simplification of and consider as a time weakening term, which weakens with

time t over a timescale t_0 since beginning slipping at t_s and restrengthens when resticking occurs, dropping a maximum σ_0. This allows for a huge numerical speedup compared with more expensive rate and state formulations, and the study of time weakening friction as well.

[12] The last term $\epsilon \nabla_{\parallel}^2 \frac{\partial S}{\partial t}$, with ϵ a small constant and $\nabla_{\parallel}^2$ the fault parallel second derivative, provides stability at the shortest wavelengths [*Langer and Nakanishi*, 1993; *Shaw and Rice*, 2000].

[13] The numerical scheme proceeds by first evolving the fault system quasistatically, taking advantage of the dependence of the fault system evolution on the total slip, rather than slip increments, on the faults. Once a desired total strain is reached, the system is switched to elastodynamic mode. The system is loaded until one point is just at the point of failure. The event evolves then under fully inertial dynamics. Once the event has stopped slipping, the waves are quenched in the system, and the system is then reloaded until the next point is just at failure.

3. Results

[14] Figure 2 shows one of the central results of this paper, plotting the distribution of sizes of events for different fault geometries as well as different frictions. The two different fault geometries are for the same slip-weakening localization, at different stages of a fault system evolution with increasing strain. We see, as has been suggested by field observations [*Stirling et al.*, 1996] an evolution from a more Gutenberg-Richter like distribution at smaller strains to a more characteristic like distribution at larger strains. We also include in this plot the distributions of segment lengths for the two geometries, shown with the dotted lines. Note that the longest events are much longer than the longest segments, so we are getting events cascading across multiple segments. Note also, interestingly, that the distribution of lengths of events is not a simple scaling of the distribution of lengths of segments. One cannot simply derive the distribution of sizes of events from the distribution of faults, as has been proposed [*Scholz*, 1998].

[15] Figure 2 also shows the result of using the same fault geometry, but different frictions. We show three different frictions, slip weakening, velocity weakening, and time weakening in this plot, shown with different colored lines. Note the only small differences in the resulting distributions of sizes of events. We have examined a wide range of frictional parameters and a variety of model generated fault systems, and found surprisingly little sensitivity in the distribution of sizes of events to the frictional instability. This is in marked contrast with the single planar fault case, in which the frictional parameters play a dominant role in the resulting distributions, particularly with respect to the small events [*Shaw and Rice*, 2000].

[16] How then is geometry impacting the distribution of sizes of events? One key hypothesis has been that segments fail as units. This is a central assumption in many attempts to understand the Gutenberg-Richter law, and a key ingredient in many hazard estimates. A further question, with major implications for hazard estimates, is the degree to which dynamic events cascade across segments,
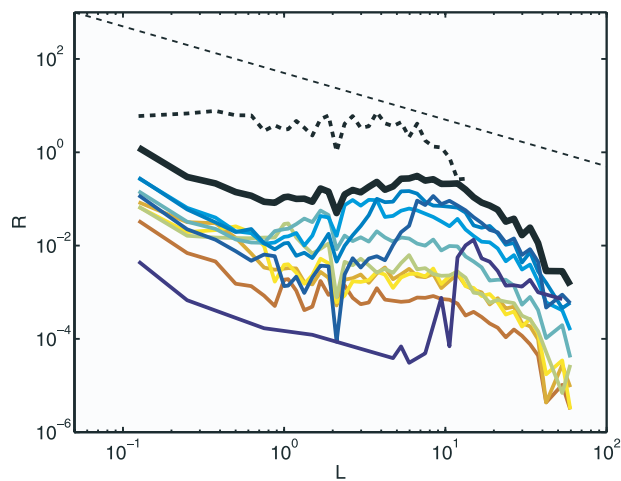
Figure 3. Distribution of lengths of events disaggregated for different segment lengths. Note peaks in the distributions at lengths corresponding to the logarithmically binned segments lengths $L = .22, .38, .66, 1.2, 2.0, 3.5, 6.1, 10, 18$, shown from red colored to blue colored lines, respectively. The thick black line shows the total summed over all segment bin lengths. The dotted line is the distribution of segment lengths. The thin black dashed line has a slope of -1.

giving multisegmented ruptures. Figure 3 plots the distribution of sizes of events grouped by segment length. We measure the length of each segment, and record at each point on the segment all the sizes of the events during which that point broke. We then sum over all the points for segments with similar lengths, to end up with a distribution of sizes of events for which segments having that length participated in. The total summed over all faults is shown with the thick black line. This curve is slightly different than previous curves in Figure 2 in that whereas before we were counting each event of a given length once, now we are counting each event at each point where it broke, so events are weighted by their length, and thus the slope of the curve is reduced by 1 relative to the previous plots. (This is done to make connection to what one would see paleoseismically at a trench). The disaggregated curves, plotted with a colorscale changing from red to blue with increasing segment length, show a number of interesting features. First, the distributions of sizes of events show peaks at the segments they are occurring on. Second, while the peaks occur at the segment lengthscales, we do see events which are much smaller and also much longer than the segment lengthscale. Thus both partial segment breakage and multiple segment cascades are occurring. Finally, the distribution of small event on segments appear to follow the same power law distribution as the aggregate. Taken together, these features support a modified form of the segmentation hypothesis, whereby segments both break in power law small events and occasionally participate

in cascading larger events, but also predominantly break as a unit.

References

Bouchon, M., and D. Streiff (1997), Propagation of a shear crack on a nonplanar fault: A method of calculation, *Bull. Seismol. Soc. Am.*, *87*, 61.

Carlson, J. M., and J. S. Langer (1989), Mechanical model of an earthquake fault, *Phys. Rev. A*, *84*, 6470.

Dieterich, J. H. (1994), A constitutive law for the rate of earthquake production and its application to earthquake clustering, *J. Geophys. Res.*, *99*, 2601.

Harris, R. A., and S. M. Day (1999), Dynamic 3D simulations of earthquake on en echelon fault, *Geophys. Res. Lett.*, *26*, 2089.

Harris, R. A., R. J. Archuletta, and S. M. Day (1991), Fault steps and the dynamic rupture process: 2-D numerical simulations of a spontaneously propagating shear fracture, *Geophys. Res. Lett.*, *18*, 893.

Heslot, F., T. Baumberger, B. Perrin, B. Caroli, and C. Caroli (1994), Creep, stick-slip, and dry-friction dynamics: Experiments and a heuristic model, *Phys. Rev. E*, *49*, 4973.

Kame, N., and T. Yamashita (1997), Dynamic nucleation process of shallow earthquake faulting in a fault zone, *Geophys. J. Int.*, *128*, 204.

Lachenbruch, A. (1980), Frictional heating, fluid pressure, and the resistance to fault motion, *J. Geophys. Res.*, *85*, 6097.

Langer, J. S., and H. Nakanishi (1993), Models of rupture propagation: 2. Two dimensional model with dissipation on the fracture surface, *Phys. Rev. E*, *48*, 439.

Lyakhovsky, V., Y. Ben-Zion, and A. Agnon (2001), Earthquake cycle, fault zones, and seismicity patterns in a rheologically layered lithosphere, *J. Geophys. Res.*, *106*, 4103.

Melosh, H. J. (1996), Dynamical weakening of faults by acoustic fluidization, *Nature*, *379*, 601.

Mora, P., and D. Place (1999), The weakness of earthquake faults, *Geophys. Res. Lett.*, *26*, 123.

Myers, C. H., B. E. Shaw, and J. S. Langer (1996), Slip complexity in a crustal plane model of an earthquake fault, *Phys. Rev. Lett.*, *77*, 972.

Rice, J. R. (1999), Flash heating at asperity contacts and rate-dependent friction, *Eos Trans. AGU*, *80*(46), Fall Meet. Suppl., Abstract S21D-05.

Scholz, C. H. (1998), A further note on earthquake size distributions, *Bull. Seismol. Soc. Am.*, *88*, 1325.

Shaw, B. E. (1995), Frictional weakening and slip complexity on earthquake faults, *J. Geophys. Res.*, *100*, 18,239.

Shaw, B. E. (1997), Modelquake in the two dimensional wave equation, *J. Geophys. Res.*, *102*, 27,367.

Shaw, B. E. (1998), Far field radiated energy scaling in elastodynamic earthquake fault models, *Bull. Seismol. Soc. Am.*, *88*, 1457.

Shaw, B. E., and J. R. Rice (2000), Existence of continuum complexity in the elastodynamics of repeated fault ruptures, *J. Geophys. Res.*, *105*, 23,791.

Shaw, B. E., and C. H. Scholz (2001), Slip-length scaling in large earthquakes: Observations and theory and implications for earthquake physics, *Geophys. Res. Lett.*, *28*, 2995.

Sibson, R. H. (1973), Interactions between temperature and pore fluid pressure during earthquake faulting and a mechanism for partial or total stress relief, *Nature Phys. Sci.*, *243*, 66.

Spyropoulos, C., C. H. Scholz, and B. E. Shaw (2002), Transition regimes for growing crack populations, *Phys. Rev. E*, *65*, 056105.

Stirling, M. W., S. G. Wesnousky, and K. Shimazaki (1996), Fault trace complexity, cumulative slip, and the shape of the magnitude-frequency distribution for strike-slip faults: A global survey, *Geophys. J. Int.*, *124*, 833.

Tullis, T. E., and D. L. Goldsby (2003), Flash melting of crustal rocks at almost seismic slip rates, *Eos Trans. AGU*, *84*(47), Fall Meet. Suppl., Abstract S51B-05.

————————————
B. E. Shaw, Lamont-Doherty Earth Observatory, Palisades, NY 10964, USA. (shaw@ldeo.columbia.edu)

Electronic Supplement

Bulk Equations

The equations of motion we are solving are as follows. Dimensionlesss variables are used throughout to achieve a minimal parameterization. In the 2D scalar bulk, we have

$$\frac{\partial^2 u}{\partial t^2} = \nabla^2 u + (w - u) - \eta \frac{\partial u}{\partial t} + \nabla \cdot \mathbf{M} \ , \quad (1)$$

where u is displacement, t is time, $\nabla^2 = \frac{\partial^2}{\partial x^2} + \frac{\partial^2}{\partial y^2}$ is the two-dimensional Laplace operator representing the horizontal elastic coupling of the displacement field, and the $w - u$ term represents the vertical coupling to the lower ductile layer. Lengths are scaled in the problem so that the brittle layer depth is set to unity. The ductile layer is slowly stretched, loading the upper brittle layer and moving as

$$w = \nu y t \qquad (2)$$

with $\nu \ll 1$ the tectonic loading rate. The dissipation constant η damps the waves, and is used to mimic geometrical spreading effects which are otherwise much weaker in our 2D model as compared to 3D. The final term is the body forces arising from the fault dislocation openings $\mathbf{M}$

$$\mathbf{M} = \delta u \bigg|_{\Gamma} \ . \qquad (3)$$

The boundary condition on the faults Γ are that the normal strain equals the traction

$$\nabla u \cdot \perp \Gamma \bigg|_{\Gamma} = \phi \ . \qquad (4)$$

All of the nonlinearity in the problem is contained in the friction ϕ, which has a stick-slip form, resisting motion up to some threshold value, and acting against motion when sliding occurs. We represent the stick-slip by

$$\phi = \Phi(\frac{\partial S}{\partial t'}, t' \le t) H(\frac{\partial S}{\partial t}) \qquad (5)$$

where Φ is a scalar frictional strength, $S = |\mathbf{M}|$ is the slip and $\partial S / \partial t$ is the slip rate on the fault, and H is the antisymmetric step function

$$H = \begin{cases} \frac{\hat{\partial S}}{\partial t} & \frac{\partial S}{\partial t} \ne 0; \\ |H| < 1 & \frac{\partial S}{\partial t} = 0 \ . \end{cases} \qquad (6)$$

which represents the stick-slip nature of the friction, being multivalued at zero slip rate, and opposing motion in the $\frac{\hat{\partial S}}{\partial t}$ unit direction when slipping.

What remains a big open question for earthquakes, is what is the frictional strength ϕ. The main text discusses this frictional strength in further detail.

For numerical simplicity, we restrict the faults segments Γ to be perpendicular to the stretching direction y. We also discretize the equations onto a rectangular grid, and use a second order finite difference approximation of the continuum equations. Parameters used in the simulations shown, unless otherwise indicated, are: fault parameters $\beta = 1.3$, $\varepsilon = 2$; domain parameters $\delta_x = .125$, $\delta_y = .125$, $L_x = 84$, $L_y = 12$; bulk parameter $\eta = .2$; friction parameters $\alpha = 3$, $\gamma = .1$, $\sigma_0 = .3$, $t_0 = .2$, $\epsilon = .003$. Periodic boundary conditions in both directions are used.